Proceedings Paper:

Terzioglu, F. orcid.org/0000-0002-2639-2992, Rongong, J.A. and Lord, C. (2022) The effect of particle surface roughness on granular energy dissipation performance. In: Proceedings of the 24th International Congress on Acoustics. 24th International Congress on Acoustics, 24-28 Oct 2022, Gyeongju, South Korea. International Congress on Acoustics .

PROCEEDINGS of the
24th International Congress on Acoustics

October 24 to 28, 2022 in Gyeongju, Korea

The effect of particle surface roughness on granular energy dissipation performance

Furkan TERZIOGLU[1]; Jem A. RONGONG[2]; Charles E. LORD[3]

[1] Department of Mechanical Engineering, University of Sheffield, United Kingdom

[2] Department of Mechanical Engineering, University of Sheffield, United Kingdom

[3] Department of Mechanical Engineering, University of Sheffield, United Kingdom

ABSTRACT

Granular materials can be effectively utilised to reduce structure-borne noise and structural vibrations. However, since granular damping shows non-linear characteristics and is affected by several different parameters such as particle shape, a granular damper should be designed considering the factors that may change granular energy dissipation behaviour. The particles used in a granular damper are generally assumed as having a certain geometric shape. However, particle surfaces can deviate from the pre-defined shape due to manufacturing limitations or wear during operation. This experimental study investigates the extent of particle surface distortion on the energy dissipation performance of a partially filled granular damper exposed to harmonic excitation parallel to the direction of gravity. The effect of the particle surface is evaluated over a range of amplitude and frequency conditions. Moulded and 3D printed spherical particles are used to indicate smooth and non-smooth particle shapes, respectively. In order to quantify the particle surface smoothness, a set of surface roughness measurements is carried out. A dissipated power measurement test rig is used to assess dissipative performances of smooth and non-smooth spherical particle types in a cylindrical granular damper enclosure.

Keywords: granular damping, surface roughness, 3D printed particle

1. INTRODUCTION

Relatively small particles placed in a cavity on a vibrating structure produce energy dissipation via inter-particle interactions. This passive damping technique is called as “granular damping” or “particle damping” (1). Because of its effectiveness even under challenging environmental conditions, it has been employed in a wide range of engineering applications to attenuate noise and reduce vibrations (2–5). Nevertheless, it shows significant non-linear characteristics, and the design of granular dampers depends on many different factors such as clearance, excitation direction, particle shape.

A granular damper is practically a combination of impact damper and friction damper. Thus, it exhibits the typical dynamic properties of both dampers (6) by dissipating the vibrational energy through inelastic collisions and frictional interactions within the granular medium. But, the sensitivity of granular damper performance to coefficient of restitution and friction coefficient of individual particles is somewhat found to be relatively low compared to the other damper parameters (7–9) as there is an apparent trade-off between the two principal dissipation sources.

However, these findings are based on the assumption of absolute smooth particle surfaces (in particle-level simulations) although the surface roughness is one of the primary factors that directly affects the individual particle coefficient of restitution and coefficient of friction (10,11). As the wear (due to long operational duration) or the manufacturing inconsistencies can cause a level of surface roughness on the employed particles in the damper, this therefore can lead the possible performance changes in granular damper designs.

This paper focuses determining the particle surface roughness effect on the overall granular damper

[1] fterzioglu1@sheffield.ac.uk
[2] j.a.rongong@sheffield.ac.uk
[3] c.lord@sheffield.ac.uk

effectiveness conducting experimental studies. Two different particle surface types, whose surface characteristics are quantified using surface roughness measurements, are used for this investigation. The individual contact properties of particles are measured to verify the mentioned numerical findings of the previous studies considering the contact property changes along with the surface roughness.

2. SMOOTH AND NON-SMOOTH PARTICLES

In order to examine the effect of particle surface roughness on the granular energy dissipation, a moulded smooth particle and a 3D printed non-smooth particle were employed throughout this study. These particles are illustrated in Figure 1. The material properties of these particles are based on acrylic-based polymer, and the nominal particle diameters are 5 mm.

(a) (b)

Figure 1 – Investigated spherical particles: (a) smooth and (b) non-smooth.

As can be seen in Figure 1, the smooth particle surface seems perfectly spherical whilst the non-smooth particle has apparent manufacturing marks. To determine the difference between the two surfaces, a set of surface roughness measurements was carried out using the Alicona InfiniteFocus optical surface measurement machine. The example surface pictures of particle types captured by the machine are demonstrated in Figure 2.

(a) (b)

Figure 2 – Particle surfaces: (a) smooth and (b) non-smooth.

To quantify each particle surface roughness, the average mean roughness parameter (Ra) was computed integrating the depth profile of a selected path line on a particle surface, $z(x)$, as:

$$\mathrm{Ra} = \frac{1}{L_{\mathrm{path}}} \int_{0}^{L_{\mathrm{path}}} \left| z(x) \right| dx \tag{1}$$

where L_{path} is the total length of the selected path line. The measurement results are summarised in Table 1.

Table 1 – Measured average mean surface roughness values.

Particle no	**Smooth particle, Ra [μm]**	**Non-smooth particle – perpendicular to fibres, Ra [μm]**	**Non-smooth particle – on fibre, Ra [μm]**
1	0.15 ± 0.02	11.22 ± 0.58	0.34 ± 0.04
2	0.16 ± 0.02	12.47 ± 0.24	0.34 ± 0.03
3	0.17 ± 0.04	11.66 ± 1.04	0.38 ± 0.02
4	0.15 ± 0.02	11.56 ± 0.80	0.35 ± 0.05
5	0.17 ± 0.01	12.96 ± 0.69	0.33 ± 0.04
Average	0.16	11.97	0.35

As can be seen from Table 1, 5 different specimens were considered for each particle type in the measurements to obtain an average surface characteristic for the particle types. For each specimen, 4 different path lines were constructed to determine the variation in the results depending on the selection of path position on the specimen surfaces. Although the directional orientation of this path selection does not matter for the smooth particle, two different path directions were particularly used for the non-smooth particle to establish its surface roughness because of the effect of printed fibres. The selection of path direction can be clearly seen in Figure 3 with the exemplified path depth functions.

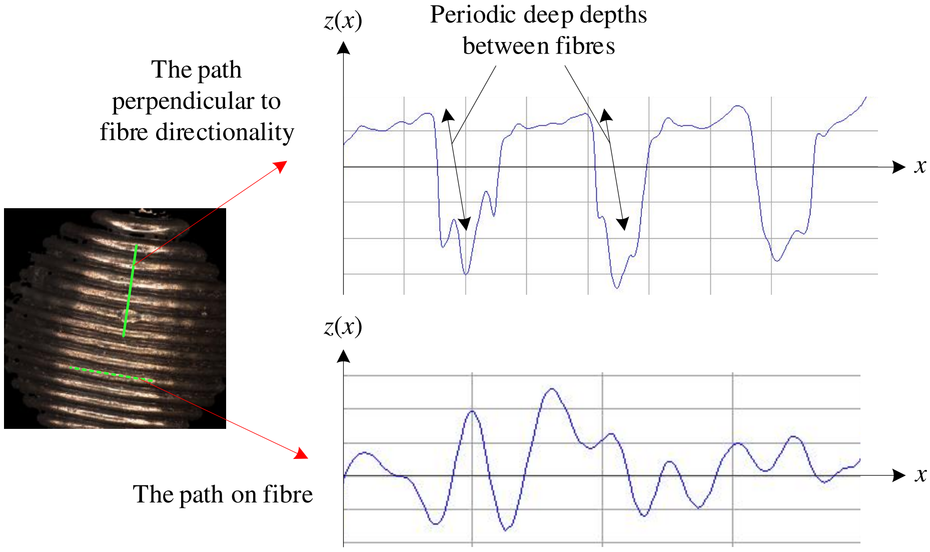

Figure 3 – Demonstration of different path directions on the non-smooth particle.

The surface roughness difference between the two different path directions of non-smooth particle is apparent as can be seen in Table 1. The smooth particle has very low surface roughness compared to the non-smooth particle.

It should be noted that the sphericity of particles is maintained. Although the non-smooth particle has relatively large surface roughness values when the fibre-perpendicular paths are considered, the ratio of its average mean surface roughness to the diameter is about 0.2%. Hence, for the granular energy dissipation characteristics of non-spherical particle shapes, the authors address the previous studies (12–14).

3. COLLISIONAL PROPERTIES OF INDIVIDUAL PARTICLES

To show the effect of surface roughness on the normal collisional behaviour of each introduced particle, a simple experimental drop test rig was proposed as shown in Figure 4. In this test rig, the tested particle is released from an unknown height to the base plate, and it should be allowed to make at least 3 successive impacts with the flat plate surface within the measurement sequence. The force history of each impact is captured by the force transducer mounted between the base plate and a fixed ground.

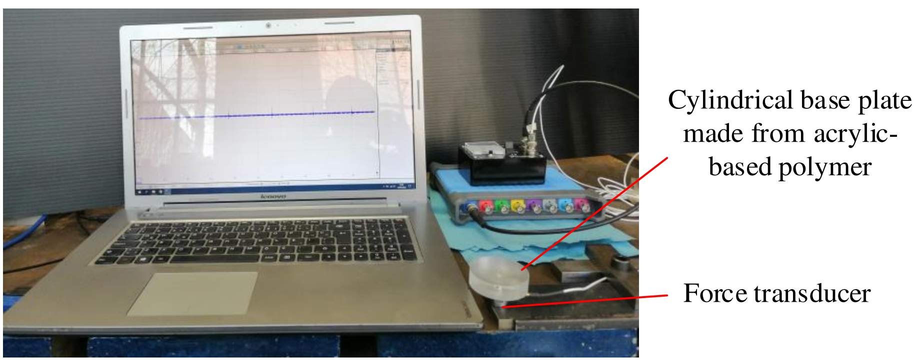

Figure 4 – Simple drop test rig.

A sample measurement which shows 3 subsequent impacts of a smooth particle with the base is illustrated in Figure 5. A basic algorithm was used to identify the impacts. It also calculates the times between the impacts, $T_{1\text{-}2}$ and $T_{2\text{-}3}$, and the contact durations of impacts, ΔT_1, ΔT_2 and ΔT_3.

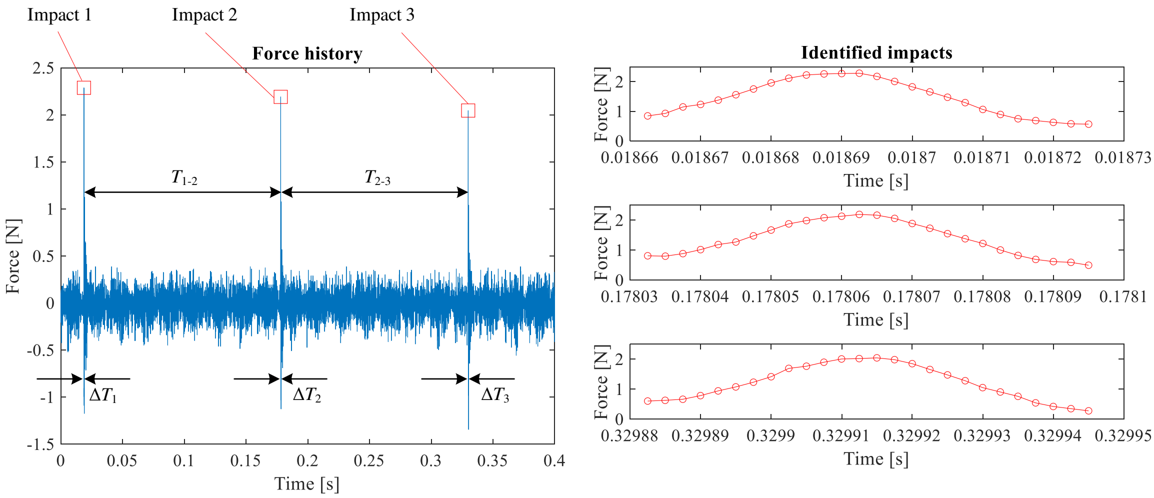

Figure 5 – A sample drop test measurement.

In this experimental rig, it was aimed to measure and compare the impact-based dissipation level, i.e., coefficient of restitution (COR), and the contact stiffness of the smooth and non-smooth particles. The determination of these properties was carried out utilising the theoretical approach presented by Nagurka and Huang (15). Nagurka and Huang (15) have basically modelled the bouncing behaviour of a spherical ball (i.e., particle) on a flat surface as a single-degree-freedom system as shown in Figure 6. In this model, m_{particle} is the individual particle mass; k_{contact} is the contact stiffness; c_{contact} is the contact damping coefficient determined by the contact damping ratio, ζ_{contact} which is a function of COR (16).

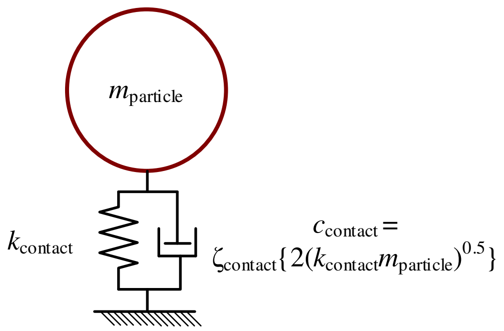

Figure 6 – Single-degree-of-freedom model of an individual impact.

Employing this model, COR, e_{contact} is obtained using the time gaps between the captured impacts in the proposed test rig as:

$$e_{\text{contact}} = T_{2-3} / T_{1-2} \tag{2}$$

The contact stiffness is determined using the measured COR as:

$$k_{\text{contact}} = \frac{m_{\text{particle}}}{\left(\Delta T_{\text{contact}}\right)^2}\left[\pi^2 + \ln^2\left(e_{\text{contact}}\right)\right] \tag{3}$$

where the average contact duration can be found by,

$$\Delta T_{\text{contact}} = \left(\Delta T_1 + \Delta T_2 + \Delta T_3\right)/3 \tag{4}$$

The measured properties are shown in Figure 7 depending on the impact velocity obtained as $2T_{1\text{-}2}/g$ where g is the gravity. Note that the experienced impact velocities are much smaller than the yield velocity. Therefore, there is no certain effect of impact velocity on the measured COR values.

It is apparent from the presented results that the smooth and the non-smooth particles exhibit very different collisional properties. The mean COR is about 0.91 and the mean contact stiffness is approximately 3.9×10^5 N/m for the smooth particle whilst they respectively are 0.83 and 2.1×10^5 N/m for the non-smooth particle. This shows that increase in particle surface roughness reduces COR and contact stiffness. It should be noted that this result is consistent with literature (10).

It should be noted that sampling rate, base plate vibration after the loss of contact and particle releasing are the most significant factors that affect the accuracy of impact capturing in this test rig. It was observed that the detected contact durations were very sensitive to these issues, and, therefore the contact stiffness values had large uncertainties. However, as the time gaps between subsequent impacts are insensitive to mis-determination of contact durations, it can be said that the estimation of COR with this method is reliable despite its simplicity.

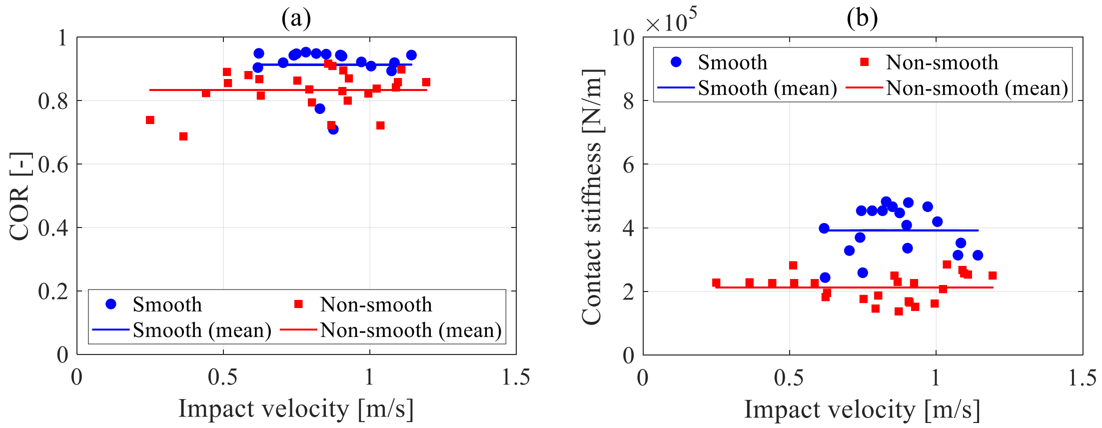

Figure 7 – Measured collisional properties: (a) COR and (b) contact stiffness.

4. GRANULAR ENERGY DISSIPATION EFFECTIVENESS OF PARTICLES

The experimental test rig used in this study to measure the dissipated energy of a vibrated granular medium is shown in Figure 8. It was proposed as analogue to the pioneering Yang's work (17). As can be realised from Figure 8, no main structure is present in this test rig. In this way, the dissipated energy effectiveness can be obtained as independent from the host structure dynamics, and, therefore consistent comparisons can be conducted at any frequency and amplitude.

The used cylindrical enclosure has the inside diameter of 40 mm and the void height of 40 mm. This provided 0.47 volume fill ratio as 358 particles were employed in the damper enclosure for both smooth and non-smooth particle types. The enclosure material is the same as the particles. It should be also noted that the first natural frequency of damper enclosure is higher than 1200 Hz.

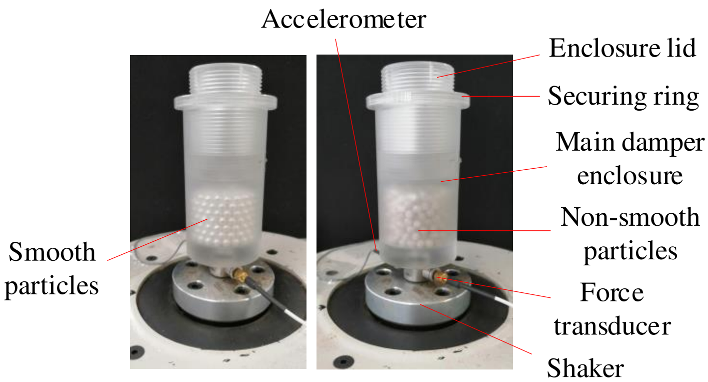

Figure 8 – Granular energy dissipation measurement rig with smooth and non-smooth particles.

The theoretical equations and detailed explanations to calculate the dissipated energy using this test rig can be found elsewhere (7). The computation procedure is basically based on simultaneous measurement of developing acceleration and force while the shaker applies harmonic excitation to the damper enclosure. Thus, the acceleration and force signals were captured for each excitation condition (i.e., amplitude and frequency) considered here using the mounted transducers on the damper enclosure outer surface as shown in Figure 8.

For each measurement, the granular medium was allowed to reach the steady-state condition while it was driven by vibration. The acceleration and force signals were then captured for 5 seconds to obtain the average dissipated energy achieved by the damper. This averaged measurement provided to eliminate possible uncertainties that can occur in a single vibration cycle measurement. The used sampling rate for the signal acquisition was 40 kHz for accurate measurement of the corresponding signals.

To allow consistent comparisons, the granular damping efficiency parameter (18) was used:

$$\text{Damping efficiency} = E_{\text{dissipated}}\omega^2 / \left(2\Gamma g\right)^2 M_{\text{particle}} \quad (5)$$

where $E_{\text{dissipated}}$ is the average dissipated energy in a vibration cycle by the damper; ω is the excitation frequency in rad/s; Γ is the non-dimensional acceleration amplitude determined dividing the excitation acceleration amplitude by the standard gravity, g; and M_{particle} is the total particle mass employed.

The granular damping efficiency levels of smooth and non-smooth particles are shown in Figure 9 for different excitation cases in order to determine the effect of surface roughness on the damping under a variety of dynamic conditions of granular medium. For example, the peak in Figure 9a and the largest peak in Figure 9b are the results of optimum collective collision condition where the granular medium exhibits the onset of bouncing bed phase. Besides, the smaller peak in Figure 9b and the peaks in Figure 9c and Figure 9d are responsible to the optimum condition of fluidisation motional behaviour in the granular medium. More detailed explanations on the relation between the dynamic granular motion and the achieved granular damping effectiveness can be found in elsewhere (19,20).

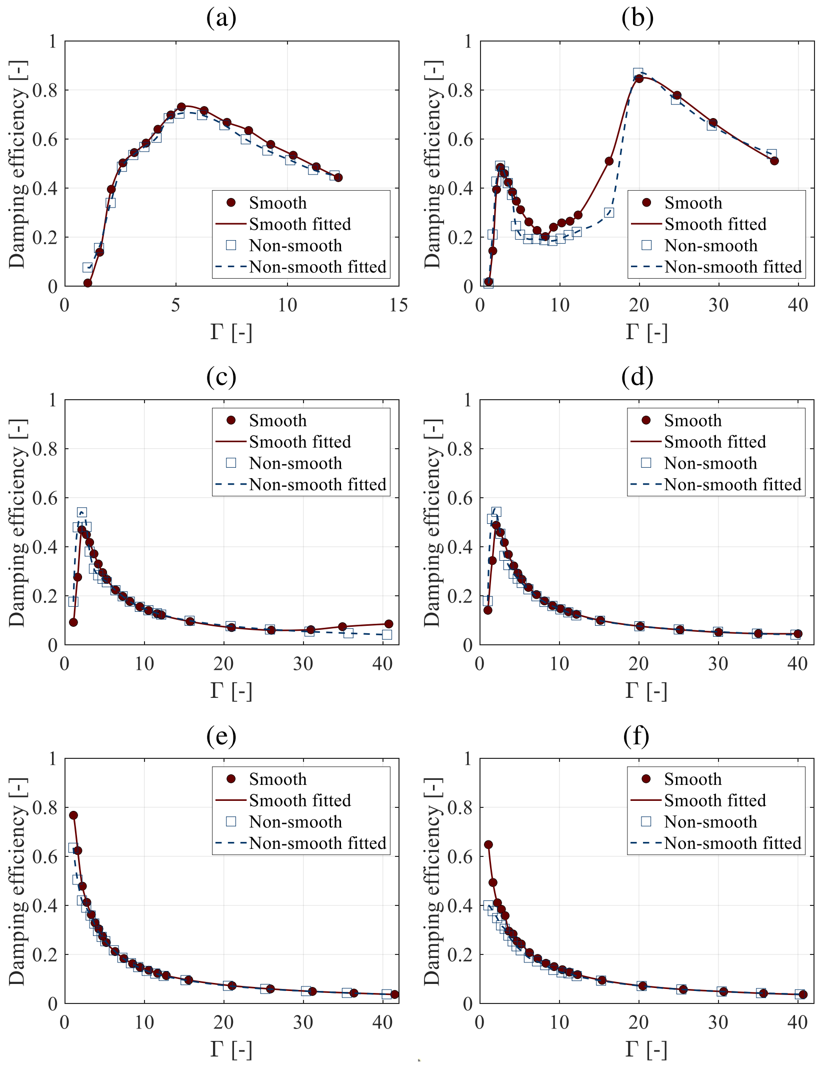

Figure 9 – Damping efficiency comparisons for varying vibration amplitudes at (a) 20 Hz, (b) 40 Hz, (c) 125 Hz, (d) 160 Hz, (e) 320 Hz and (f) 625 Hz.

As can be seen in Figure 9, the granular damping efficiency levels of smooth and non-smooth particles are very similar to each other along the whole vibration amplitude axis at each excitation frequency investigated although there are significant differences between them in terms of surface roughness (see Table 1) and individual collisional properties (see Figure 7). Both particle types captured the same dynamic characteristic behaviours for each excitation case as the same volume fill ratio was used for both. This also showed that the obtained ratio of the average mean surface roughness to the diameter for the non-smooth particle type (i.e., 0.2%) does not affect the overall spherical particle shape.

It is somewhat surprising that the smooth particle exhibits more effective granular damping for most of the excitation cases despite its higher COR value than the non-smooth particle. It can be explained that the smooth particles generate more intensive inter-particle interactions (i.e., larger relative velocity and larger deformation) within the shaken granular medium which results more efficient energy dissipation by the particles. This finding also confirms the previous results obtained from the numerical parameter sensitivity analyses of granular dampers (7,9). It should be noted that although it was not measured in this study it has been reported elsewhere that the coefficient of friction grows with increasing surface roughness (11). Therefore, this can be regarded as another factor that reduces intensity of generated interactions in the granular medium, and, therefore the granular damping effectiveness decreases as also shown in another parametric study (8).

5. CONCLUSIONS

The presented experimental study has investigated the effect of particle surface roughness in a granular damper subjected to axial vertical harmonic vibrations. Two apparently different spherical particle surface types were considered for this comparative study: smooth and non-smooth. The quantifying properties of investigated particle types were identified by conducting surface roughness measurements and simple drop tests. This study has revealed that the smooth particle generally provides more effective energy dissipation in granular dampers. However, the associated difference between the employed particle types has been found very small even though the particle types has exhibited significantly different individual collisional properties. The results have also indicated that the amplitude and frequency dependent granular damping characteristic, which most-likely depends on the dynamic motional behaviour of granular medium, is insensitive to the particle surface roughness as the used surface roughness level has not considerably affected the overall particle shape and the volume fill ratio. Therefore, there is no major effect of surface roughness on granular damping performance if the particle surface distortion does not create a certain different geometry from the original particle shape.

REFERENCES

1. Panossian H V. Structural damping enhancement via non-obstructive particle damping technique. J Vib Acoust. 1992;114(1):101–5.
2. Panossian H V. Non-obstructive particle damping: New experiences and capabilities. In: 49th AIAA/ASME/ASCE/AHS/ASC Structures, Structural Dynamics and Materials Conference. Schaumburg, Illinois; 2008.
3. Simonian SS. Particle damping applications. In: 45th AIAA/ASME/ASCE/AHS/ASC Structures, Structural Dynamics and Materials Conference. Palm springs, California; 2004. p. 4145–61.
4. Hu L, Shi Y, Yang Q, Song G. Sound reduction at a target point inside an enclosed cavity using particle dampers. J Sound Vib. 2016;384:45–55.
5. Xu Z, Yu Wang M, Chen T. A particle damper for vibration and noise reduction. J Sound Vib. 2004;270(4–5):1033–40.
6. Mao K, Wang MY, Xu ZZ, Chen T. Simulation and characterization of particle damping in transient vibrations. J Vib Acoust. 2004;126(2):202–11.
7. Wong CX, Daniel MC, Rongong JA. Energy dissipation prediction of particle dampers. J Sound Vib. 2009;319(1–2):91–118.
8. Lu Z, Masri SF, Lu X. Parametric studies of the performance of particle dampers under harmonic excitation. Struct Control Heal Monit. 2011;18(1):79–98.
9. Wang Y, Liu B, Tian A, Tang W. Experimental and numerical investigations on the performance of particle dampers attached to a primary structure undergoing free vibration in the horizontal and vertical directions. J Sound Vib. 2016;371:35–55.
10. Sandeep CS, Luo L, Senetakis K. Effect of grain size and surface roughness on the normal coefficient of restitution of single grains. Materials (Basel). 2020;13(4).
11. Li X, Dong M, Jiang D, Li S, Shang Y. The effect of surface roughness on normal restitution coefficient, adhesion force and friction coefficient of the particle-wall collision. Powder Technol. 2020;362:17–25.

12. Terzioglu F, Rongong JA, Lord CE. The dissipative characteristics of oblate particles in granular dampers. In: Proceedings of the International Conference on Structural Dynamic , EURODYN. 2020. p. 4851–66.
13. Pourtavakoli H, Parteli EJR, Pöschel T. Granular dampers: Does particle shape matter? New J Phys. 2016;18(7).
14. Sánchez M, Carlevaro CM, Pugnaloni LA. Effect of particle shape and fragmentation on the response of particle dampers. J Vib Control. 2014;20(12):1846–54.
15. Nagurka M, Huang S. A mass-spring-damper model of a bouncing ball. In: Proceedings of the American Control Conference. Boston, Massachusetts; 2004. p. 499–504.
16. Schwager T, Pöschel T. Coefficient of restitution for viscoelastic spheres: The effect of delayed recovery. Phys Rev E - Stat Nonlinear, Soft Matter Phys. 2008;78(5):1–12.
17. Yang MY. Development of master design curves for particle impact dampers. The Pennsylvania State University; 2003.
18. Sack A, Heckel M, Kollmer JE, Zimber F, Pöschel T. Energy dissipation in driven granular matter in the absence of gravity. Phys Rev Lett. 2013;111(1):1–5.
19. Terzioglu F, Rongong JA, Lord CE. Motional phase maps for estimating the effectiveness of granular dampers. Mech Syst Signal Process. 2022;Submitted.
20. Terzioglu F, Rongong JA, Lord CE. Construction of motional phase maps for granular dampers. In: INTER-NOISE 2022 - 51st International Congress and Exposition on Noise Control Engineering: Noise Control in a More Sustainable Future. Glasgow; 2022.